Available online at www.sciencedirect.com
SCIENCE DIRECT
Journal of Catalysis 238 (2006) 369–381
JOURNAL OF CATALYSIS
www.elsevier.com/locate/jcat

Enantioselective epoxidation of unfunctionalized olefins catalyzed by the Mn(salen) catalysts immobilized in the nanopores of mesoporous materials

Huidong Zhang, Yanmei Zhang, Can Li *

State Key Laboratory of Catalysis, Dalian Institute of Chemical Physics, Chinese Academy of Sciences, Dalian, 116023, China

Received 8 November 2005; revised 8 December 2005; accepted 13 December 2005

Available online 27 January 2006

Abstract

Three Mn(salen) catalysts were immobilized in nanopores or on external surface of mesoporous materials via phenyl sulfonic groups with different linkage lengths. The influence of the axial linkage length and the nanopores or external surface of supports on the catalytic performance of the heterogeneous Mn(salen) catalysts was investigated in detail. The *ee* values increase with increasing linkage length for the Mn(salen) catalysts immobilized in nanopores but remain almost unchanged for those catalysts anchored on the external surface. The *ee* values obtained for the Mn(salen) catalysts immobilized in nanopore increase with decreasing nanopore size and they are generally higher than those of the same catalysts anchored on the external surface of support. Modification of the nanopore surface by methyl groups improves the reaction performance for the asymmetric epoxidation. The confinement effect originating from nanopores not only enhances the chiral recognition of the chiral catalyst, but also restricts the rotation of the intermediate in nanopores, enhancing the asymmetric induction and giving higher *ee* values than those obtained for the same catalysts anchored on the external surface.

Keywords: Heterogeneous catalysis; Chiral catalysis; Enantioselective; Asymmetric catalysis; Epoxidation; Sulfonic; Immobilization; Grafting; Unfunctionalized olefin; Mn(salen) complexes; Confinement effect

1. Introduction

Due to the great importance of the chiral compounds in the manufacture of drugs, vitamins, fragrances, and optical material, the synthesis of chiral building blocks has attracted special attention. Chiral epoxides are among the most important intermediates that can be readily transfered into various chiral compounds via regioselective ring-opening or functional transfer reactions. Chiral Mn(salen)Cl complexes [1,2] exhibit excellent activity and enantioselectivity for the homogeneous asymmetric epoxidation of various unfunctionalized olefins [3–6].

But homogeneous catalytic reactions always entail difficulties in separation and recycling of catalysts and purification of products, hindering practical application of homogeneous asymmetric epoxidation as well as many other homogeneous reactions. The heterogeneous catalytic systems can potentially solve these problems [7–9]. In addition to these merits, the solid surface or the nanopores of the supports may provide an unexpected effect on asymmetric catalytic performance for heterogeneous asymmetric epoxidation. Various strategies for immobilizing Mn(salen) complexes have been reported, including covalent grafting of Mn(salen) on mesoporous materials [10–15] or carbon materials [16], ion-exchange of Mn(salen) into layered double hydroxides [17–20] or Al-MCM-41 [21,22], encapsulation in zeolite [23], and co-condensation of VO(salen) into periodic mesoporous materials [24,25]. A few heterogeneous catalysts have exhibited higher *ee* values than the homogeneous ones for asymmetric epoxidation. However, the effects of the nanopores or surface of supports and the linkages of the catalysts on activity, chemical selectivity, and enantioselectivity have seldom been systemically investigated for heterogeneous asymmetric epoxidation.

Recently, we reported [26] that chiral Mn(salen) complexes can be successfully immobilized onto inorganic mesoporous materials via a phenyl sulfonic group, and that these catalysts have higher *ee* values than the homogeneous ones for the asym-

* Corresponding author. Fax: +86 411 84694447.
E-mail address: canli@dicp.ac.cn (C. Li).
URL: http://www.canli.dicp.ac.cn (C. Li).

0021-9517/$ – see front matter
doi:10.1016/j.jcat.2005.12.023

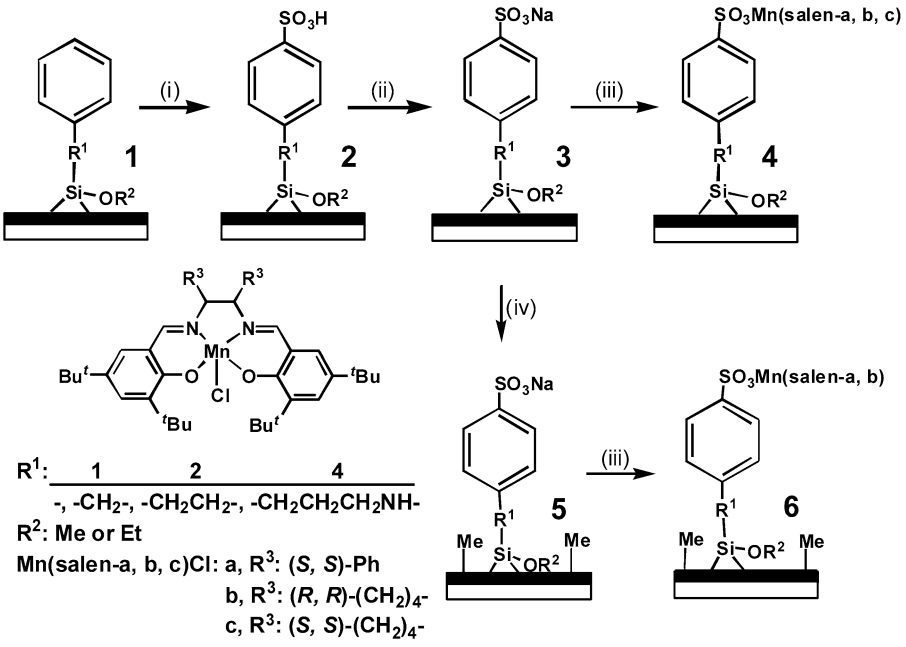

Scheme 1. Preparation of the heterogeneous chiral Mn(salen) catalysts. Conditions: (i) 10% fuming sulfuric acid, 40 °C, 2 h, (ii) $NaHCO_3$, room temperature, 3 h; (iii) Mn(salen)Cl, ethanol, reflux, 5 h; (iv) $MeSi(OMe)_3$, toluene, reflux.

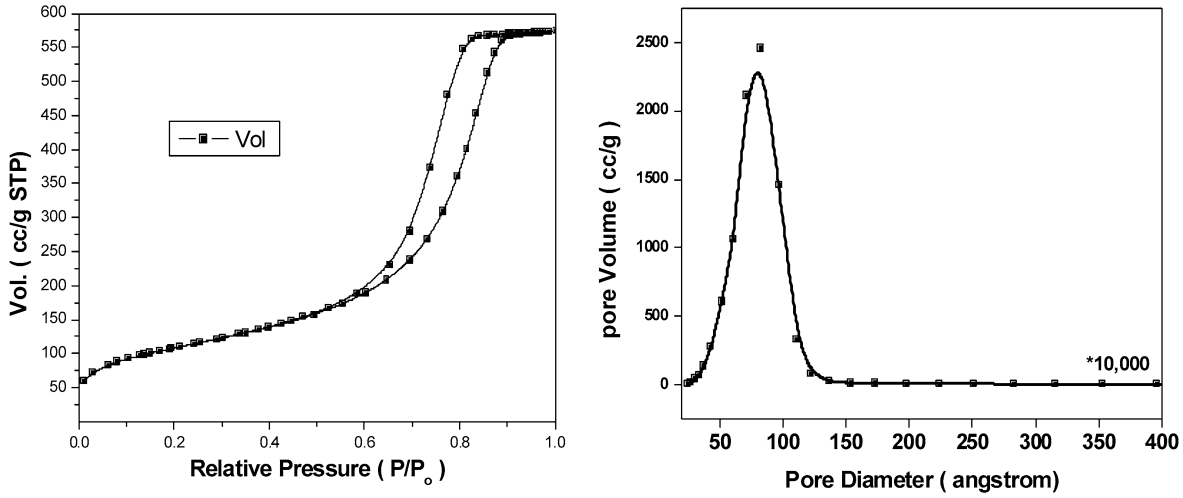

Fig. 1. The nitrogen adsorption–desorption isotherms of AS(9.7) (activated silica) (left) and pore size distribution curve of AS(9.7) calculated from the desorption branch (right).

metric epoxidation of some olefins. To investigate the influence of linkage length and nanopores or external surfaces of supports on reaction performance, chiral Mn(salen) complexes were immobilized into the nanopores or onto the external surface of mesoporous materials via a phenyl sulfonic group with varying linkage lengths. It was found that the *ee* values increase with increasing the linkage length in nanopores but remain constant on the external surface. *Ee* values also increase with decreasing nanopore size, which are generally greater than that of the same catalyst anchored on the external surface. The modification of nanopore surface by methyl groups further improves the reaction performance for the asymmetric epoxidation. The confinement effect originating from nanopores can enhance the chiral recognition of chiral catalysts and restrict the rotation of intermediates, resulting in increasing *ee* values with the increasing length of linkage groups for the catalysts immobilized in the nanopores rather than on the external surface.

2. Experimental

2,4-di-*tert*-Butylphenol, hexamethylenetetramine (HMTA), L-(+)-tartaric acid, D-(−)-tartaric acid, *cis*/*trans*-1,2-diaminocyclohexane, 1,2-dihydronaphthalene, $PhSi(OEt)_3$, $PhCH_2Si(OEt)_3$, (*S*,*S*)-1,2-diphenylethylenediamine, 3-chloroperoxybenzoic acid (*m*-CPBA), 4-phenylpyridine *N*-oxide (PPNO), $PhCH_2CH_2Si(OMe)_3$, and $PhNH(CH_2)_3Si(OMe)_3$ were purchased from Acros and used as received. Three salen ligands (Scheme 1) were synthesized and characterized as described previously [27,28]. Activated silica (pore size of 9.7 nm with sharp pore distribution; Fig. 1), SBA-15 (pore size 7.6 nm),

and MCM-41 (pore sizes 2.7 and 1.6 nm) were used as supports and abbreviated as AS(9.7), SBA(7.6), MCM(2.7), and MCM(1.6), respectively. Three representative olefins – monosubstituted styrene, disubstituted 1,2-dihydronaphthalene, and trisubstituted 1-phenylcyclohexene – were chosen as model substrates to test the heterogeneous Mn(salen) catalysts. The racemic epoxides were prepared by epoxidation of the corresponding olefins by *m*-CPBA in $CHCl_3$ at 0 °C [14] and confirmed by gas chromatography–mass spectroscopy (GC–MS). Epoxides were analyzed by GC–MS, and the yield (with *n*-nonane as internal standard) and the *ee* values were determined by GC (6890N, Agilent) using a chiral column (Agilent).

All Fourier transform infrared (FTIR) spectra were collected on a FTIR spectrometer (Nicolet Nexus 470) with a resolution of 4 cm^{-1} and 64 scans in the region of 4000–400 cm^{-1}. IR spectra of the free complexes and the supported complexes were recorded by preparing samples as KBr pellets and self-supporting wafers, respectively. The ultraviolet–visible light (UV–vis) spectra were recorded on a JASCO V-550 spectrometer. The solution of Mn(salen)Cl in CH_2Cl_2 (about 1.0 mM) was poured into a 1-cm quartz cell for UV–vis adsorption with CH_2Cl_2 as a reference. Diffuse reflectance UV–vis spectra of the solid samples were recorded using a spectrophotometer with an integrating sphere using $BaSO_4$ as a reference. X-Ray diffraction (XRD) patterns were recorded on a Rigaku D/Max 3400 powder diffraction system using Cu-K_α radiation over the range $0.5 \leqslant 2\theta < 10°$. Thermogravimetric analysis (TGA) was performed on a Perkin–Elmer Pyris Diamond TG instrument at a temperature range of 20–900 °C at a heating rate of 5 °C/min under an air flow. The nitrogen sorption experiments were performed at 77 K on an ASAP 2000 system in static measurement mode. The samples were degassed at 100 °C for 5 h before the measurements were obtained. The pore size distribution curves were obtained from a desorption isotherm using the BJH method.

2.1. Preparation of heterogeneous Mn(salen) catalysts

2.1.1. Supports grafted by organic sulfonic sodium

Pure siliceous support [AS(9.7), SBA(7.6), MCM(2.7), or MCM(1.6), 9 g] was dehydrated at 125 °C under 0.01 Torr for 4 h before the addition of the fresh $PhSi(OEt)_3$, $PhCH_2Si(OEt)_3$, $PhCH_2CH_2Si(OMe)_3$, or $PhNHCH_2CH_2CH_2Si(OMe)_3$ (21 mL) in dry toluene (450 mL). The resulting mixture was stirred for 1 h at room temperature, then refluxed for 18 h at 120 °C under Ar, during which time the various phenyl groups were grafted onto the supports [29]. After being cooled, filtrated, and washed thoroughly with toluene, the solid was dried at 60 °C under reduced pressure overnight to obtain the supports grafted with phenyl groups, abbreviated as Ph-R^1-support (**1**) (Scheme 1).

The Ph-R^1-support (**1**, 3 g) was dehydrated at 125 °C under 0.01 Torr for 4 h, then cooled to 40 °C under Ar atmosphere. Fuming sulfuric acid (10%, 10 mL) was added to the solid, and the resulting mixture was stirred at 40 °C for 2 h [30] (Scheme 1), during which time the phenyl groups were converted to phenyl sulfonic groups. The solid was filtrated under reduced pressure, washed with distilled water until the pH was 7, and washed three times with 1,4-dioxane, three times with ethanol, and then again with distilled water to obtain the $PhSO_3H$-R^1-support (**2**). To this wet solid **2**, distilled water (20 mL) containing $NaHCO_3$ (0.33 g, 3.9 mmol) was added to neutralize the $PhSO_3H$ groups; this mixture was stirred for 3 h at room temperature. The solid was filtrated and washed to neutral to produce the $PhSO_3Na$-R^1 support in the form of a white powder (**3**).

2.1.2. Supports modified with methyl groups

The $PhSO_3Na$-R^1-AS(9.7) samples (**3**, 3 g) were dehydrated at 125 °C under 0.01 Torr for 4 h, then combined with fresh $MeSi(OMe)_3$ (3 mL) in dry toluene (50 mL) (Scheme 1). The resulting mixture was stirred for 1 h at room temperature, then refluxed at 120 °C under Ar for 18 h, during which time the methyl groups were grafted onto the mesoporous materials. After being cooled, filtrated, and washed thoroughly with toluene, the solid was dried at 60 °C under reduced pressure overnight to obtain the $PhSO_3Na$-R^1-AS(9.7)(CH_3) (**5**) as a white powder (Scheme 1).

2.1.3. Grafting chiral Mn(salen) catalysts onto mesoporous supports

The grafting of Mn(salen) complexes was done by refluxing mixture **3** or **5** (1.0 g) with Mn(salen)Cl (1.0 mmol) in ethanol (60 mL) for 5 h [12,14]. The solid was filtrated and washed thoroughly with ethanol, then CH_2Cl_2, to eliminate all the Mn(salen) complexes adsorbed on the supports. The CH_2Cl_2 filtrates were detected by UV–vis spectroscopy until no peaks were detected (using CH_2Cl_2 as a reference). After drying, the heterogeneous Mn(salen) catalysts $PhSO_3Mn$(salen-a, b, c)-R^1-support (**4**) and $PhSO_3Mn$(salen-a,b)-R^1-AS(9.7)(CH_3) (**6**) were obtained as brown powders (Scheme 1).

Once the heterogeneous Mn(salen) catalysts (**4** or **6**) are prepared, the chlorine ions in the filtrate can be separated out and confirmed by a HNO_3–$AgNO_3$ aqueous solution. But no characteristic reaction was observed for the addition of HNO_3–$AgNO_3$ aqueous solution to Mn(salen)Cl or CH_2Cl_2 solvent under identical conditions. This demonstrates that Mn(salen) is immobilized on supports via an ion-exchange mode. The pure siliceous support without phenyl groups was also sulfonated and neutralized according to Scheme 1. Then the support was used to graft Mn(salen)Cl catalyst under the same conditions. But the support quickly turned white after a washing with CH_2Cl_2, and no Mn element was detected in the support by ICP analysis. This confirms that the Mn(salen) complexes are anchored onto supports via the phenyl sulfonic group. The Mn(salen) adsorbed on the supports can be easily removed by washing with CH_2Cl_2.

2.2. Asymmetric epoxidation

To quantitatively compare the catalytic performance, the amount of heterogeneous catalysts was normalized based on the same amount of Mn(salen). Dichloromethane was used

as the optimal solvent, and *n*-nonane was used as an internal standard because of its stability, inertness, and easy handling (b.p. 151 °C). A typical epoxidation reaction [14] was performed in a stirred solution of olefin (1 mmol) in CH_2Cl_2 (3 mL) containing *n*-nonane (1.0 mmol), PPNO as an axial additive (0.38 mmol), Mn(salen) catalysts (0.015 mmol, 1.5 mol%, based on Mn element), and NaClO aqueous solution (pH = 11.5, 0.55 M, 3.64 mL, 2 eqv.) at 0 °C (styrene) or 20 °C (other substrates) for 6 or 24 h. After the reaction, the organic layer was concentrated and purified by flash chromatography for homogeneous systems or filtered to separate catalysts for heterogeneous systems.

3. Results

3.1. Catalyst characterizations

The IR spectra of the AS(9.7) grafted with various phenyl groups are shown in Fig. 2. The IR bands at 1490, 1496, and 1479 cm^{-1} can be attributed to the vibrations of aromatic phenyl rings grafted on the support. The IR bands at 1431 and 1454 cm^{-1} are due to C–H deformation vibrations of alkyl groups (R^1 and R^2 in Scheme 1). The IR bands at 1500 and 1605 cm^{-1} (N–H deformation vibrations) can be attributed to the –NH– groups attached to phenyl groups (curve d). The increased length of the linkage groups also results in stronger bands of C–H stretching vibrations near 3000 cm^{-1}. The FTIR spectra indicate successful grafting of the phenyl groups on the supports. The IR spectra of the heterogeneous Mn(salen) catalyst are shown in Fig. 3. The IR bands of Ph-2-AS(9.7) at 1496 and 1456 cm^{-1} are due to the stretching vibrations of C=C bonds of the phenyl ring and the deformation vibrations of the C–H bond of the alkyl groups, respectively. The sulfonation of the phenyl groups on AS(9.7) gives new bands at 1409, 1388, and 1433 cm^{-1}, which are related to the stretching vibrations of the $–SO_2–$ groups. Grafting Mn(salen) complex onto the modified support gives a new characteristic band of Mn(salen) at 1535 cm^{-1}, indicating the presence of Mn(salen) catalyst on the support.

The IR spectra of the heterogeneous Mn(salen) catalyst whose support was modified with methyl groups are shown in Fig. 4. The IR spectrum of the support modified by methyl groups shows three C–H stretchings at 2979, 2952, and 2850 cm^{-1} due to the methyl groups. The Mn(salen) grafted onto the modified support shows a new characteristic IR band of Mn(salen) complex at 1535 cm^{-1}. The IR spectra confirm the successful modification of the mesoporous support with methyl groups and the grafting of Mn(salen) complex onto the supports.

Fig. 5 shows the UV–vis spectra of the heterogeneous Mn(salen-a) catalysts. The Mn(salen-a)Cl complex gives two characteristic bands at 446 and 332 nm (curve a). The modified supports, Ph-2-AS(9.7), $PhSO_3Na$-2-AS(9.7), and $PhSO_3Na$-2-AS(9.7)(CH_3), present only the bands of phenyl groups of 200–300 nm in UV–vis spectra (curves b–d). After grafting of Mn(salen-a) complex onto these supports, the characteristic bands of Mn(salen-a) complex reappear in their spectra,

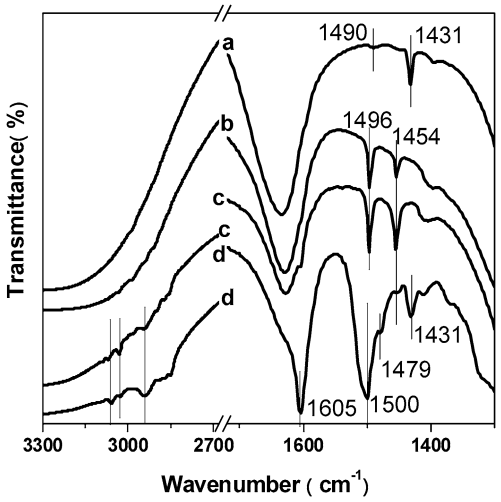

Fig. 2. The FT-IR spectra of (a) Ph-AS(9.7), (b) Ph-1-AS(9.7), (c) Ph-2-AS(9.7), and (d) Ph-4-AS(9.7).

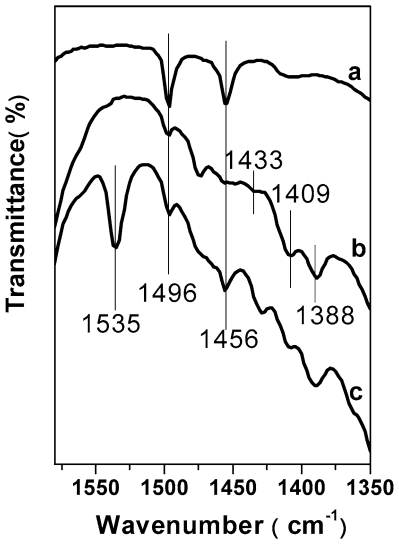

Fig. 3. The FT-IR spectra of (a) Ph-2-AS(9.7), (b) $PhSO_3Na$-2-AS(9.7), and (c) $PhSO_3Mn$(salen-a)-2-AS(9.7).

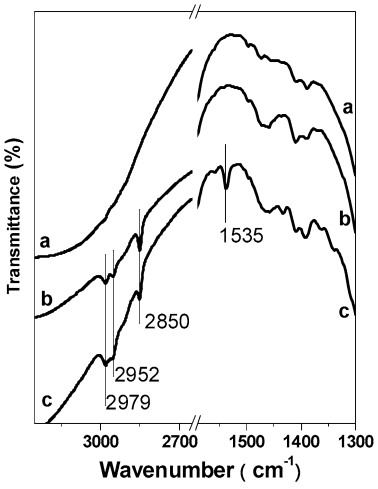

Fig. 4. The FT-IR spectra of (a) $PhSO_3Na$-2-AS(9.7), (b) $PhSO_3Na$-2-AS(9.7)(CH_3), and (c) $PhSO_3Mn$(salen-b)-2-AS(9.7)(CH_3).

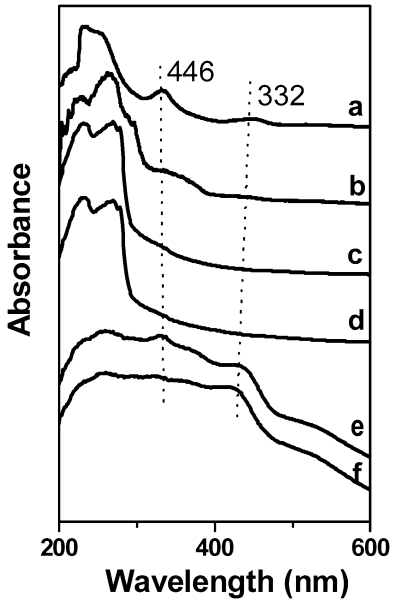

Fig. 5. The UV–vis spectra of (a) Mn(salen-a)Cl, (b) Ph-2-AS(9.7), (c) $PhSO_3Na$-2-AS(9.7), (d) $PhSO_3Na$-2-AS(9.7)(CH_3), (e) $PhSO_3Mn$-(salen-a)-2-AS(9.7), and (f) $PhSO_3Mn$(salen-a)-2-AS(9.7)(CH_3).

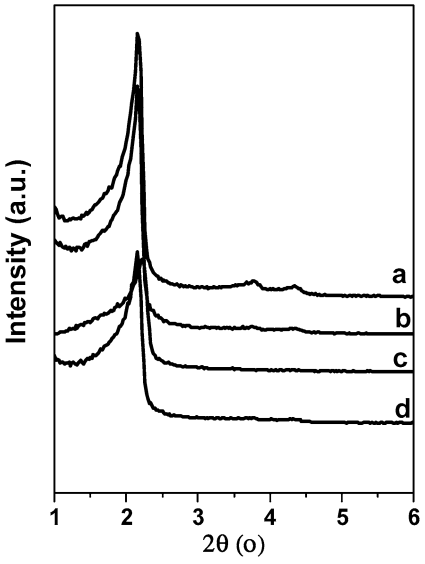

Fig. 6. The PXRD patterns of (a) MCM(1.6), (b) Ph-2-MCM(1.6), (c) $PhSO_3Na$-2-MCM(1.6), and (d) $PhSO_3Mn$(salen-b)-2-MCM(1.6).

but the bands are shifted from 446 and 332 nm to 432 and 329 nm for $PhSO_3Mn$(salen-a)-2-AS(9.7) (curve e) and to 425 and 324 nm for $PhSO_3Mn$(salen-a)-2-AS(9.7)(CH_3) (curve f), indicating the electrostatic interaction between the supports and the immobilized Mn(salen) complex. This further confirms the successful immobilization of Mn(salen) complex on the supports.

The powder XRD patterns of the modified supports and the heterogeneous catalyst are shown in Fig. 6. The powder XRD patterns of Ph-2-MCM(1.6) and $PhSO_3Na$-2-MCM(1.6) show a similar periodic structure to that of MCM-41. The mesoporous support with the grafted Mn(salen) complex retains the good periodic structure.

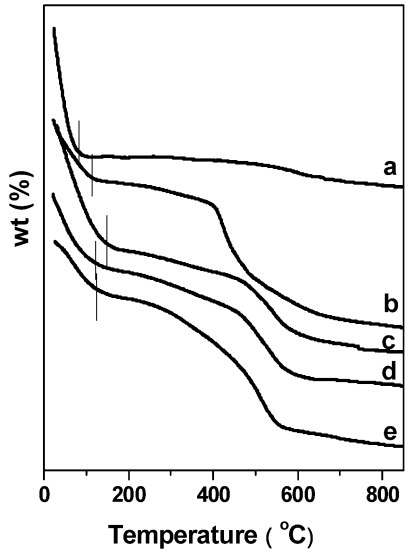

Fig. 7. The TG curves of (a) AS(9.7), (b) Ph-AS(9.7), (c) $PhSO_3Na$-AS(9.7), (d) $PhSO_3Na$-AS(9.7)(CH_3), and (e) $PhSO_3Mn$(salen-a)-AS(9.7)(CH_3).

The TG curves of heterogeneous Mn(salen) catalyst are shown in Fig. 7. The TG curves of AS(9.7) and $PhSO_3Na$-AS(9.7) show a sharp decrease before T_{H_2O} (the temperatures for the complete desorption of water from the samples). Ph-AS(9.7) and $PhSO_3Na$-AS(9.7)(CH_3) show decreased slopes of curves for the desorption of water. These slopes are directly related to the polarity of the support surface. Table 1 also shows a semiquantitative amount of various organic groups grafted on AS(9.7) based on their gravity losses. The Mn content in the catalysts estimated by TG is 0.027 mmol/g, close to the value of 0.021 mmol/g analyzed by ICP. The actual amount of Mn(salen) grafted on the supports is in the range of 0.01–0.04 mmol/g detected by ICP-AES (based on Mn).

The sizes of the solvated Mn(salen)Cl complexes are estimated as 2.05 nm × 1.77 nm for Mn(salen-a)Cl and 2.05 nm × 1.61 nm for Mn(salen-b)Cl by MM2 based on the minimized energy. The immobilization of these complexes into the nanopores of supports requires supports with large pore sizes. The nitrogen sorption results (Table 2) show that Ph-2-AS(9.7) has smaller nanopore size, surface area, and pore volume than AS(9.7) (entries 1 and 2); therefore, the phenyl groups are located mainly in the nanopores of AS(9.7). The prepared heterogeneous catalyst $PhSO_3Mn$(salen-b)-2-AS(9.7)(CH_3) shows a further decrease in nanopore size (from 7.7 to 5.9 nm), surface area (from 289 to 248 m^2/g), and pore volume (from 0.62 to 0.39 cm^3/g) compared with Ph-2-AS(9.7) (entries 2 and 3). These decreased surface area and pore volume further suggest that Mn(salen) complexes are immobilized mainly into the nanopores of AS(9.7), because the surface area of AS(9.7) is contributed mainly by the nanopore surface [15]. Similarly, the Mn(salen) complexes are also immobilized mainly into the nanopores of SBA(7.6) and MCM(2.7). The nitrogen sorption results show that $PhSO_3Na$-MCM(1.6) has smaller nanopore size and pore volume than MCM(1.6) (entries 4 and 5), but the immobilization of Mn(salen-b) complex onto $PhSO_3Na$-MCM(1.6) hardly changes the pore size and pore volume (en-

Table 1
The amounts of various organic groups grafted on AS(9.7) estimated by TG[a]

Sample	T_{H_2O}[b] (°C)	W_1[c] (%)	W_2[d] (%)	ΔW[e] (%)	Groups	mmol/g[f]
AS(9.7)	93	91.37	89.66	1.71	–	–
Ph-2-AS(9.7)	105	96.42	87.52	8.90	Ph	0.621
$PhSO_3Na$-2-AS(9.7)	125	92.27	84.01	8.26	$PhSO_3Na$	0.572
$PhSO_3Na$-2-AS(9.7)(CH_3)	114	96.34	87.61	8.73	Me	0.531
$PhSO_3Mn$(salen-b)-2-AS(9.7)(CH_3)	115	97.34	87.04	9.60	Mn(salen-b)	0.027

[a] TG was performed from 20 to 900 °C at a heating rate of 5 °C/min under air flow.
[b] The inflexion temperature for the complete desorption of water from the samples.
[c] The residual mass percent at T_{H_2O}.
[d] The residual mass percent at 850 °C.
[e] $\Delta W\ (\%) = W_1\ (\%) - W_2\ (\%)$, responding to the loss of organic groups.
[f] The amount of the organic groups grafted on the support.

Table 2
The results of N_2 adsorption of supports, modified supports and heterogeneous Mn(salen) catalysts[a]

Entry	Sample	Pore size[b] (nm)	S_{BET}[c] (m^2/g)	Pore volume[d] (cm^3/g)
1	Activated silica	9.7	332	0.71
2	Ph-2-AS(9.7)	7.7	289	0.62
3	$PhSO_3Mn$(salen-b)-2-AS(9.7)(CH_3)	5.9	248	0.39
4	MCM-41	1.6	553	0.56
5	Ph-MCM(1.6)	1.4	431	0.26
6	$PhSO_3Mn$(salen-b)-MCM(1.6)	1.4	403	0.27

[a] The samples were degassed at 100 °C for 5 h.
[b] Pore size based on the desorption data using BJH method.
[c] Surface based on multipoint BET method.
[d] Pore volume based on the desorption data of BJH method.

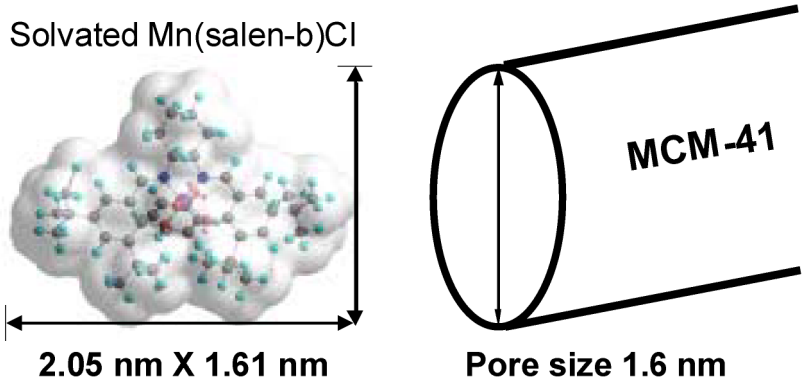

Scheme 2. The sizes of the solvated Mn(salen-b)Cl and nanopores of MCM-41 (1.6 nm).

tries 5 and 6). This is because the solvated Mn(salen)Cl complexes are too large to be accommodated into the nanopores of MCM(1.6) (Scheme 2); therefore, Mn(salen) complexes are immobilized mainly onto the external surface of MCM(1.6).

3.2. The different linkage lengths

The results for the asymmetric epoxidation of styrene catalyzed by homogeneous and heterogeneous Mn(salen-a) catalysts are listed in Table 3. 4-Phenylpyridine *N*-oxide (PPNO) as an axial additive is usually used to adjust the electronic and steric property of chiral Mn(salen) complexes in asymmetric epoxidation [2,4]. The homogeneous catalyst Mn(salen-a)Cl gives the stoichiometric conversion and chemical selectivity with PPNO for the epoxidation of styrene, but the same catalyst without PPNO produces benzaldehyde and acetophenone as byproducts under the same catalytic conditions. However, the *ee* values remain almost unchanged for the two cases (entries 1 and 2). The addition of PPNO can improve the catalytic activity of $PhSO_3Mn$(salen-a)-AS(9.7) (entries 3 and 4). When the length of linkage groups R^1 of $PhSO_3Mn$(salen-a)-R^1-AS(9.7) is increased from one-bond long to five-bonds long, the catalytic reaction performance (including conversion, chemical selectivity, and *ee* values) improves (entries 4–7). The *ee* values obtained for the heterogeneous catalysts (i.e., 58%) are comparable to that of the homogeneous catalyst (58%).

The modification of the nanopore surface with methyl groups can slightly improve enantioselectivity but greatly improve conversion and chemical selectivity for the asymmetric epoxidation of styrene (entries 8–11). For example, conversion

Table 3
Asymmetric epoxidation of styrene catalyzed by homogeneous and heterogeneous Mn(salen-a) catalysts[a]

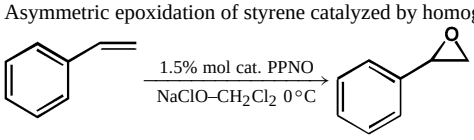

Entry	Catalyst	T (h)	Conversion (%)	Selectivity[b] (%)	ee[c] (%)
1	Mn(salen-a)Cl[d]	6	81	88	56
2	Mn(salen-a)Cl	6	100	100	58
3	$PhSO_3$Mn(salen-a)-AS(9.7)[d]	24	3	–	–
4	$PhSO_3$Mn(salen-a)-AS(9.7)	24	31	63	49
5	$PhSO_3$Mn(salen-a)-1-AS(9.7)	24	36	67	53
6	$PhSO_3$Mn(salen-a)-2-AS(9.7)	24	38	84	57
7	$PhSO_3$Mn(salen-a)-4-AS(9.7)	24	42	90	58
8	$PhSO_3$Mn(salen-a)-AS(9.7)(CH_3)	24	27	68	50
9	$PhSO_3$Mn(salen-a)-1-AS(9.7)(CH_3)	24	79	86	56
10	$PhSO_3$Mn(salen-a)-2-AS(9.7)(CH_3)	24	100	95	59
11	$PhSO_3$Mn(salen-a)-4-AS(9.7)(CH_3)[e]	24	100	96	59
12	$PhSO_3$Mn(salen-a)-MCM(1.6)	24	55	62	39
13	$PhSO_3$Mn(salen-a)-1-MCM(1.6)	24	63	64	40
14	$PhSO_3$Mn(salen-a)-2-MCM(1.6)	24	73	65	39
15	$PhSO_3$Mn(salen-a)-4-MCM(1.6)	24	78	74	40

[a] Reactions were performed in CH_2Cl_2 (3 mL) with styrene (1.0 mmol), n-nonane (1.0 mmol), PPNO (0.38 mmol), catalysts (0.015 mmol, 1.5 mol%) and NaClO (pH = 11.5, 0.55 M, 3.64 mL) at 0 °C.
[b] Benzaldehyde and acetophenone as byproducts.
[c] (S)-configuration form.
[d] Without PPNO.
[e] Heterogeneous catalyst containing 0.75 mol% Mn(salen-a).

Table 4
The asymmetric epoxidation of 1,2-dihydronaphthalene catalyzed by homogeneous and heterogeneous Mn(salen-b) catalysts[a]

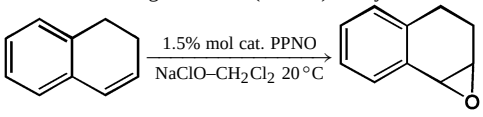

Entry	Catalyst	T (h)	Conversion (%)	ee[b] (%)
1	Mn(salen-b)Cl	6	75	72
2	Mn(salen-b)Cl[c]	6	65	55
3	$PhSO_3$Mn(salen-b)-AS(9.7)	24	69	58
4	$PhSO_3$Mn(salen-b)-1-AS(9.7)	24	71	62
5	$PhSO_3$Mn(salen-b)-2-AS(9.7)	24	73	66
6	$PhSO_3$Mn(salen-b)-4-AS(9.7)	24	68	68
7	$PhSO_3$Mn(salen-b)-AS(9.7)(CH_3)	24	72	68
8	$PhSO_3$Mn(salen-b)-1-AS(9.7)(CH_3)	24	74	70
9	$PhSO_3$Mn(salen-b)-2-AS(9.7)(CH_3)	24	70	72
10	$PhSO_3$Mn(salen-b)-4-AS(9.7)(CH_3)	24	74	74
11	$PhSO_3$Mn(salen-b)-MCM(1.6)	24	68	58
12	$PhSO_3$Mn(salen-b)-1-MCM(1.6)	24	68	60
13	$PhSO_3$Mn(salen-b)-2-MCM(1.6)	24	70	62
14	$PhSO_3$Mn(salen-b)-4-MCM(1.6)	24	73	63

[a] Reactions were performed in CH_2Cl_2 (3 mL) with 1,2-dihydronaphthalene (1.0 mmol), n-nonane (1.0 mmol), PPNO (0.38 mmol), catalysts (0.015 mmol, 1.5 mol%) and NaClO (pH = 11.5, 0.55 M, 3.64 mL) at 20 °C.
[b] (1S,2R)-configuration.
[c] Without PPNO.

increases from 38 to 100% after modification of the nanopores of $PhSO_3$Mn(salen-a)-2-AS(9.7) under the same conditions (entries 6 and 10). $PhSO_3$Mn(salen-a)-4-AS(9.7)(CH_3) can afford 100% conversion and 59% *ee* even when the catalyst loading is decreased to 0.75 mol% under the same conditions (entry 11). This can be explained in terms of the improved diffusion of styrene into the nanopores of AS(9.7) after modification with the methyl groups.

The Mn(salen-a) complex was also grafted onto the external surface of MCM(1.6) with various linkage groups. Increasing the lengths of the linkage groups improves conversion and chemical selectivity (entries 12–15). All of the conversions obtained for Mn(salen) catalyst immobilized on the external surface are higher than those in the nanopores of AS(9.7), but the chemical selectivities obtained for the catalyst immobilized on the external surface are lower than those in nanopores. Notably, the *ee* values are not affected by the lengths of the linkage groups and remain almost unchanged at 40% (entries 12–15), lower than the highest value of 58% obtained in the nanopores (entry 7).

The reaction results for the asymmetric epoxidation of 1,2-dihydronaphthalene catalyzed by homogeneous and heterogeneous Mn(salen-b) catalysts are compared in Table 4. Homogeneous Mn(salen-b)Cl catalyst gives an *ee* value of 55% for asymmetric epoxidation without PPNO. The addition of PPNO to the homogeneous system increases the *ee* value up to 72% (entries 1 and 2). The heterogeneous catalysts give comparable conversions to the homogeneous catalyst. The *ee* values obtained for the Mn(salen-b) catalyst immobilized in nanopores increase from 58 to 68% when the length of the linkage groups is increased from a one bond to five bonds (entries 3–6). The modification of nanopores of AS(9.7) with methyl groups also slightly increases the *ee* values with increasing linkage length

Table 5
The asymmetric epoxidation of 1-phenylcyclohexene catalyzed by homogeneous and heterogeneous Mn(salen-a) catalysts[a]

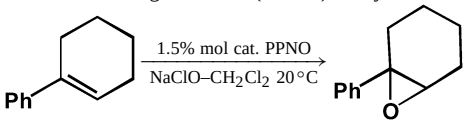

Entry	Catalysts	T (h)	Conversion (%)	ee[b] (%)
1	Mn(salen-a)Cl	6	96	84
2	$PhSO_3$Mn(salen-a)-AS(9.7)	24	86	15
3	$PhSO_3$Mn(salen-a)-1-AS(9.7)	24	87	25
4	$PhSO_3$Mn(salen-a)-2-AS(9.7)	24	92	49
5	$PhSO_3$Mn(salen-a)-4-AS(9.7)	24	89	63
6	$PhSO_3$Mn(salen-a)-AS(9.7)(CH_3)	24	88	16
7	$PhSO_3$Mn(salen-a)-1-AS(9.7)(CH_3)	24	90	28
8	$PhSO_3$Mn(salen-a)-2-AS(9.7)(CH_3)	24	93	49
9	$PhSO_3$Mn(salen-a)-4-AS(9.7)(CH_3)	24	94	65

[a] Reactions were performed in CH_2Cl_2 (3 mL) with 1-phenylcyclohexene (1.0 mmol), n-nonane (1.0 mmol), Mn(salen) catalysts (0.015 mmol, 1.5 mol%), PPNO (0.38 mmol) and NaClO (pH = 11.5, 0.55 M, 3.64 mL) at 20 °C.
[b] (R,R)-configuration.

(entries 7–10). Moreover, all of the *ee* values are higher than those of the same catalysts without surface modification under the identical reaction conditions. The catalyst $PhSO_3$Mn(salen-b)-4-AS(9.7)(CH_3) gives a comparable *ee* value of 74% to 72% for the homogeneous catalyst in the asymmetric epoxidation of 1,2-dihydronaphthalene (entries 1 and 10). When the Mn(salen-b) catalyst is immobilized onto the external surface of MCM(1.6), the *ee* values remain almost unchanged with the different linkage groups (entries 11–14). Moreover, the *ee* values obtained for the Mn(salen-b) catalyst anchored on the external surface are usually lower than those obtained for the same catalyst immobilized in nanopores.

Table 5 gives the results of the asymmetric epoxidation of 1-phenylcyclohexene catalyzed by homogeneous and heterogeneous Mn(salen-a) catalysts. The homogeneous Mn(salen-a) catalyst gives an *ee* value of 84% for the asymmetric epoxidation. The heterogeneous catalysts show similar conversions. The *ee* values increase with increasing linkage length for $PhSO_3$Mn(salen-a)-R^1-AS(9.7). When the length of linkage groups is increased from one bond to five bonds, the *ee* values increase from 15 to 63% (entries 2–5). The heterogeneous catalysts with nanopores modified with methyl groups also show that *ee* values increase with increasing length of the linkages (entries 6–9).

Mn(salen-b) catalyst immobilized into the nanopores of AS(9.7) gives the similar tendency of increasing *ee* values with increasing linkage length for the asymmetric epoxidation of 1-phenylcyclohexene (entries 2–5, Table 6). But the *ee* values remain almost unchanged with increasing linkage length when the Mn(salen-b) catalyst is immobilized on the external surface of MCM(1.6) (about 45% *ee*; entries 6–9, Table 6). Fig. 8 summarizes the *ee* values obtained for Mn(salen-b) immobilized in the nanopores of AS(9.7) and on the external surface of MCM(1.6) for the asymmetric epoxidation of 1-phenylcyclohexene. The catalysts grafted in nanopore show that the *ee* values increase with increasing linkage lengths, but the catalysts grafted on the external surface have unchanged *ee* values with increasing linkage lengths.

3.3. Nanopores with different sizes

Table 7 shows the results of the asymmetric epoxidation of styrene catalyzed by homogeneous and heteroge-

Table 6
The asymmetric epoxidation of 1-phenylcyclohexene catalyzed by homogeneous and heterogeneous Mn(salen-b) catalysts[a]

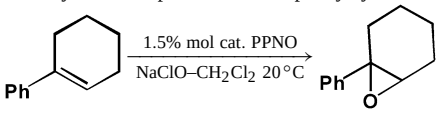

Entry	Catalyst	Add.	T (h)	Conversion (%)	ee[b] (%)
1	Mn(salen-b)Cl	PPNO	6	96	87
2	$PhSO_3$Mn(salen-b)-AS(9.7)	PPNO	24	88	14
3	$PhSO_3$Mn(salen-b)-1-AS(9.7)	PPNO	24	91	42
4	$PhSO_3$Mn(salen-b)-2-AS(9.7)	PPNO	24	93	62
5	$PhSO_3$Mn(salen-b)-4-AS(9.7)	PPNO	24	93	64
6	$PhSO_3$Mn(salen-b)-MCM(1.6)	PPNO	24	90	47
7	$PhSO_3$Mn(salen-b)-1-MCM(1.6)	PPNO	24	86	46
8	$PhSO_3$Mn(salen-b)-2-MCM(1.6)	PPNO	24	91	44
9	$PhSO_3$Mn(salen-b)-4-MCM(1.6)	PPNO	24	90	44
10	Mn(salen-b)Cl	NO	6	94	67
11	$PhSO_3$Mn(salen-b)-AS(9.7)	NO	24	84	14
12	$PhSO_3$Mn(salen-b)-4-AS(9.7)	NO	24	84	26
13	$PhSO_3$Mn(salen-b)-MCM(1.6)	NO	24	87	13
14	$PhSO_3$Mn(salen-b)-4-MCM(1.6)	NO	24	85	13

[a] Reactions were performed in CH_2Cl_2 (3 ml) with 1-phenylcyclohexene (1.0 mmol), n-nonane (1.0 mmol), Mn(salen) catalysts (0.015 mmol, 1.5 mol%), PPNO (0.38 mmol) and NaClO (pH=11.5, 0.55 M, 3.64 ml) at 20 °C.
[b] (S,S)-configuration.

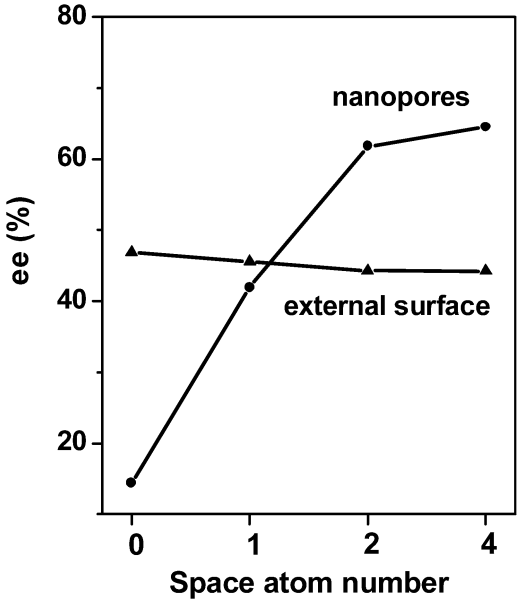

Fig. 8. The *ee* values obtained for Mn(salen-b) catalyst immobilized into nanopores of AS(9.7) and on the external surface of MCM(1.6) for the asymmetric epoxidation of 1-phenylcyclohexene.

Table 7
Asymmetric epoxidation of styrene catalyzed by homogeneous and heterogeneous Mn(salen-c) catalysts[a]

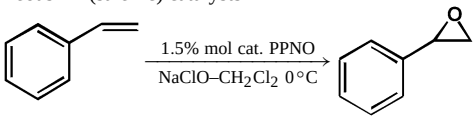

Entry	$PhSO_3Mn$(salen-c)-support	Pore size (nm)	T (h)	Conversion (%)	Selectivity[b] (%)	*ee*[c] (%)
1	Homo. Mn(salen-c)Cl	–	6	100	100	37
2	Activated Silica	9.7	24	23	79	33
3	SBA-15	7.6	24	33	80	35
4	MCM-41	2.7	24	36	83	35
5	MCM-41	1.6	24	67	75	30

[a] Reactions were performed in CH_2Cl_2 (3 mL) with styrene (1.0 mmol), *n*-nonane (1.0 mmol), PPNO (0.38 mmol), catalysts (0.015 mmol, 1.5 mol%) and NaClO (pH = 11.5, 0.55 M, 3.64 mL) at 0 °C.
[b] Benzaldehyde and acetophenone as byproducts.
[c] (*S*)-configuration.

neous Mn(salen-c) catalysts. Homogeneous Mn(salen-c)Cl catalyst gives an *ee* value of 37% for the asymmetric epoxidation of styrene (entry 1). Mn(salen-c) catalyst immobilized into nanopores of AS(9.7), SBA(7.6), and MCM(2.7) via a phenyl sulfonic group shows *ee* values comparable to that of the homogeneous catalyst (entries 2–4). Moreover, the *ee* values increase slightly with decreasing nanopore sizes in the mesoporous supports. However, under the same conditions, Mn(salen-c) anchored onto the external surface of the MCM(1.6) shows an *ee* value of 30% (entry 5), lower than the *ee* value of 35% for the catalyst immobilized in nanopores. These reaction results also show that the chemical selectivities obtained for Mn(salen) catalyst immobilized in nanopores increase with decreasing nanopore sizes and are also higher than those obtained on the external surface of MCM(1.6).

Table 8
The asymmetric epoxidation of 1-phenylcyclohexene catalyzed by homogeneous and heterogeneous Mn(salen-a) catalysts[a]

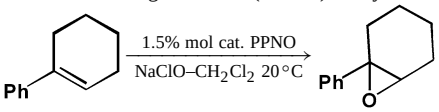

Entry	$PhSO_3Mn$(salen-a)-support	Pore size (nm)	T (h)	Conversion (%)	*ee*[b] (%)
1	Homo. Mn(salen-a)Cl	–	6	96	84
2	Activated Silica	9.7	24	86	15
3	SBA-15	7.6	24	80	18
4	MCM-41	2.7	24	71	25
5	MCM-41	1.6	24	89	31

[a] Reactions were performed in CH_2Cl_2 (3 mL) with 1-phenylcyclohexene (1.0 mmol), *n*-nonane (1.0 mmol), Mn(salen) catalysts (0.015 mmol, 1.5 mol%), PPNO (0.38 mmol) and NaClO (pH = 11.5, 0.55 M, 3.64 mL) at 20 °C.
[b] (*R*,*R*)-configuration.

These heterogeneous Mn(salen-a) catalysts were also tested for the asymmetric epoxidation of 1-phenylcyclohexene (Table 8); their conversions and enantioselectivities are lower than those of the homogeneous catalyst (entry 1). This example suggests that the phenomenon of the confinement effect improving enantioselectivity holds true for some reaction systems but not for others. Nonetheless, a significant confinement effect on catalyst performance in nanopores is seen that can either increase or decrease enantioselectivity.

3.4. Catalyst stability

The leaching of Mn(salen) complex from the heterogeneous catalyst was investigated. ICP analysis of the filtrate after a catalytic reaction shows that the loss of Mn element from the heterogeneous Mn(salen) catalyst is <3% compared with the total amount of Mn(salen) grafted in catalyst. The loss of Mn element can be due to the leaching of Mn(salen) catalyst from the supports and the loss of the hyperfine granules of the heterogeneous Mn(salen) catalysts (formed in the reaction due to stirring) during the filtration after a reaction. The conversion contribution of such little lost Mn(salen) to the catalytic epoxidation is <5% for the test of the asymmetric epoxidation of 1-phenylcyclohexene. The heterogeneous catalysts can be recycled at least five times [26]. One reason for the good stability of the heterogeneous Mn(salen) catalysts may be the effective isolation of the Mn sites on the solid support [9], whereas the Mn(salen)Cl catalysts are prone to oxidative degradation [31] and dimerization to inactive μ-oxo-Mn(IV) species [32] under homogeneous catalytic conditions.

4. Discussion

4.1. Conversions

Generally, the conversions are lower for the heterogeneous Mn(salen) catalysts than for the homogeneous catalysts, due to the difficulty in diffusion. However, the heterogeneous Mn(salen) catalysts give conversions comparable to those for the homogeneous catalysts for the asymmetric epoxidation of 1-phenylcyclohexene and 1,2-dihydronaphthalene. As for the asymmetric epoxidation of styrene, the reaction activity of the heterogeneous Mn(salen) catalysts increases after the addition of PPNO. The conversions also increase with increasing linkage lengths (Table 3). Mn(salen) catalysts immobilized on the external surface generally give higher conversions than those in the nanopores under the same catalytic conditions (Table 7). The heterogeneous Mn(salen) catalysts with supports modified with methyl groups can obviously have better conversions than those without modifications (Table 3), possibly due to the easier diffusion of olefins into the modified nanopores.

4.2. Chemical selectivities

As for the asymmetric epoxidation of styrene, benzaldehyde and acetophenone were detected as byproducts. The addition of PPNO to the heterogeneous catalytic system improves the chemical selectivity of styrene epoxide for the heterogeneous asymmetric epoxidation of styrene. The chemical selectivities also increase with increasing linkage lengths. Mn(salen) catalysts immobilized in nanopores generally give higher selectivities than those on the external surface under the same catalytic conditions. In addition, the chemical selectivities increase slightly with decreasing nanopore size of the supports in the heterogeneous Mn(salen) catalysts. The modification of the nanopores of the heterogeneous Mn(salen) catalysts with methyl groups improves chemical selectivities compared with unmodified catalysts.

4.3. Enantioselectivities

Tests for the asymmetric epoxidation of olefins over the heterogeneous Mn(salen) catalysts show that the conversions increase with increasing reaction time but that the chemical selectivities and enantioselectivities remain almost unchanged. The Mn(salen) catalyst, as the sole active center, catalyzes the asymmetric epoxidation; therefore, the enantioselectivities are independent of the conversions for the present heterogeneous catalytic system. Decreasing the nanopore sizes and modifying the nanopores with methyl groups can increase *ee* values for heterogeneous asymmetric epoxidation. Mn(salen) catalysts immobilized in nanopores generally give higher *ee* values than those anchored on the external surface. The *ee* values increase with increasing linkage lengths for the Mn(salen) catalysts immobilized in nanopores but remain almost unchanged for the same catalysts anchored on external surfaces.

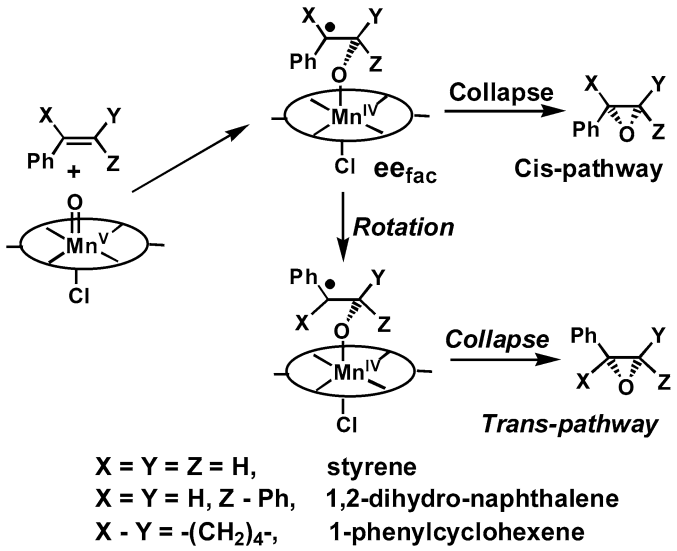

Scheme 3. The mechanism for the asymmetric epoxidation of olefins catalyzed by Mn(salen) complex [3,33,34].

4.4. The confinement effect on enantioselectivity

Scheme 3 shows the mechanism for the asymmetric epoxidation of unfunctionalized olefins catalyzed by homogeneous Mn(salen) catalyst [3,33,34]. We assumed that the mechanism on the immobilized Mn(salen) catalyst is essentially the same as that on the homogeneous catalyst. When the first C–O bond (radical intermediate) is formed, the ee_{fac} is actually determined by the steric communication between the chiral salen ligand and the olefins. As for the asymmetric epoxidation of cyclic 1,2-dihydronaphthalene and 1-phenylcyclohexene, the radical intermediate directly collapses to form the epoxide without rotation, and the observed *ee* values (ee_{obs}) are equal to the ee_{fac}. As for the asymmetric epoxidation of noncyclic olefin styrene, the intermediate will either collapse via the *cis* pathway or first rotate, then collapse via a *trans* pathway [3,34]. The observed *ee* values (ee_{obs}) can be expressed as $ee_{obs} = ee_{fac} - 2 \times (ee_{trans} \times trans\ \%)$ [3], where both ee_{fac} and the trans % are related to ee_{obs}.

PPNO can be used as a probe molecule here to investigate the influence of the confinement effect on enantioselectivity. The addition of PPNO to Mn(salen-b)Cl improves the *ee* values for the asymmetric epoxidation of 1,2-dihydronaphthalene from 55 to 72% (entries 1 and 2, Table 4) and 1-phenylcyclohexene from 67 to 87% (entries 1 and 10, Table 6), indicating that the interaction between PPNO and Mn(salen) improves ee_{fac} for the asymmetric epoxidation of the two olefins [35].

$PhSO_3$Mn(salen-b)-AS(9.7) gives similar *ee* values for the asymmetric epoxidation of 1-phenylcyclohexene with or without PPNO (entries 2 and 11, Table 6). This finding implies that there is nearly no interaction between PPNO and Mn(salen) for this catalyst. However, the addition of PPNO to $PhSO_3$Mn(salen-b)-MCM(1.6) increases the *ee* values from 13 to 47% (entries 13 and 6, Table 6), possibly due to the interaction between PPNO and Mn(salen) anchored on the external surface of MCM(1.6). The sizes of PPNO and various axial linkage groups were simulated by MM2 based on the min-

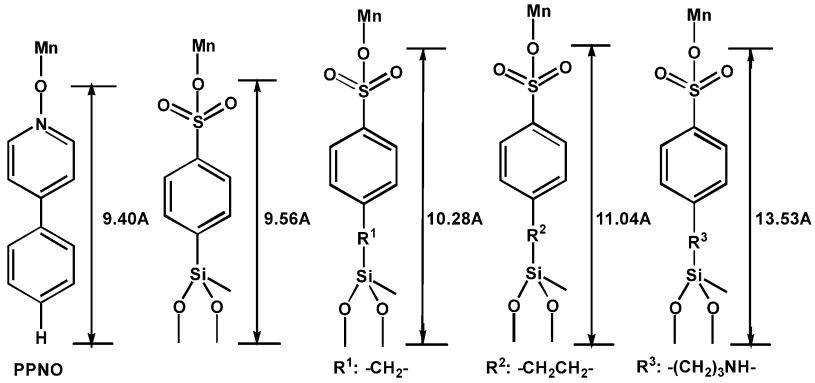

Scheme 4. The sizes of PPNO and various axial linkage groups simulated by MM2 based on the minimized energy.

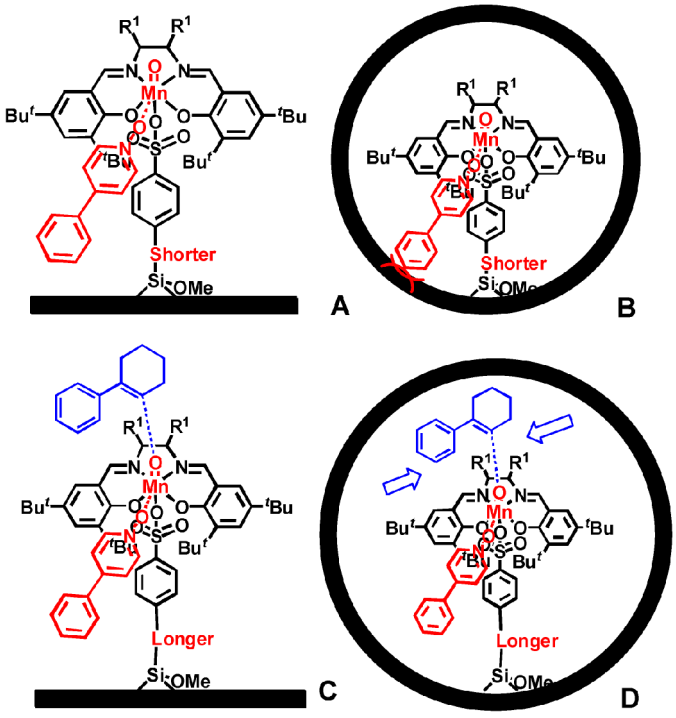

Scheme 5. The models for the interaction between PPNO and Mn(salen) immobilized on the external surface of MCM(1.6) and in the nanopores of AS(9.7) via shorter linkages (A and B). The models for the confinement effect in nanopores of AS(9.7) with longer linkages (C and D).

imized energy (shown in Scheme 4). The size of PPNO is similar to that of –O–Si–$PhSO_3$– group; therefore, the concave nanopore surface of AS(9.7) may sterically block the interaction between PPNO and Mn(salen), but the open surface of MCM(1.6) has little effect on this interaction. This supposition is also supported by the experimental results showing that the Mn(salen-a) catalyst anchored on the external surface of MCM(1.6) gives higher *ee* value than the same catalyst immobilized in various nanopores for the asymmetric epoxidation of 1-phenylcyclohexene (entries 2–5, Table 8). Schemes 5A and B give the models for the interaction between PPNO and Mn(salen) immobilized on the external surface and in the nanopores via shorter linkages.

When the linkage length is increased from one bond to two C–C bonds long (with R^1 changed from – to $–CH_2–$), the two *ee* values obtained for the Mn(salen) catalyst immobilized on the external surface of MCM(1.6) via the two linkages are almost the same (entries 6 and 7, Table 6), but the *ee* values obtained for the catalyst immobilized in nanopore of AS(9.7) are increased from 14 to 42% (entries 2 and 3, Table 6). This means that the interaction between PPNO and Mn(salen) is enhanced with increasing linkage length in the nanopores of AS(9.7), because there is sufficient space for PPNO to interact with the Mn center (Scheme 4). The similar *ee* values obtained for $PhSO_3$Mn(salen-b)-1-MCM(1.6) and $PhSO_3$Mn(salen-b)-1-AS(9.7) indicate that the concave surfaces of nanopores no longer blocks the interaction between PPNO and Mn(salen), just like the open surface of MCM(1.6).

When the linkage length is further increased (R^1 becomes $–(CH_2)_2–$ or $–(CH_2)_3NH–$), the *ee* values obtained for Mn(salen-b) catalyst immobilized in the nanopores of AS(9.7) further increase up to 65%, but the *ee* values on the external surface of MCM(1.6) remain at about 44% for the asymmetric epoxidation of 1-phenylcyclohexene (entries 4, 5, 8, and 9, Table 6). One possible explanation for this finding is that the confinement effect originating from the nanopores enhances chiral recognition between the immobilized chiral Mn(salen) catalyst and the substrate and accordingly increases the ee_{fac}. However, the open external surface of MCM(1.6) has no such confinement effect, and thus constant *ee* values are obtained. Schemes 5C and D present the proposed models for the confinement effect in nanopores with longer linkages. The confinement effect can also be supported by more experimental results. For example, the *ee* value obtained for $PhSO_3$Mn(salen-b)-4-AS(9.7) is higher than that of $PhSO_3$Mn(salen-b)-AS(9.7) for the asymmetric epoxidation of 1-phenylcyclohexene without PPNO (entries 11 and 2, Table 6). $PhSO_3$Mn(salen-b)-4-AS(9.7) also gives a higher *ee* value than $PhSO_3$Mn(salen-b)-4-MCM(1.6) under the same conditions (entries 12 and 14, Table 6).

Moreover, the *ee* values obtained for Mn(salen-a) catalyst immobilized in various nanopores via a phenyl sulfonic group increase slightly with decreasing nanopore size (entries 2–4, Table 8). This may be due to the confinement effect originating from the nanopores, which boosts the *ee* values for the asymmetric epoxidation, in which the influence of spatial constraint decreases for the mesoporous supports with pore diameters of 2.7–9.7 nm. The confinement effect, as proposed by Thomas et al. [36], could improve enantioselectivity for heterogeneous

asymmetric hydrogenation [37]. Hutchings et al. also reported that their heterogeneous catalysts showed higher *ee* values for the asymmetric aziridination of styrene [38] and hydrogenation of carbonyl- and imino-ene [39] due to the confinement effect of the supports. Here the results of the asymmetric epoxidation of 1-phenylcyclohexene clearly show that the confinement effect originating from nanopores enhances chiral recognition of the chiral catalyst and accordingly increases enantioselectivity.

As for the asymmetric epoxidation of styrene, PPNO improves conversion and chemical selectivity, but does not affect enantioselectivity (58 vs 56%; entries 1 and 2, Table 3). The Mn(salen) catalysts immobilized in the nanopores exhibit higher *ee* values than those on the external surface for the asymmetric epoxidation of styrene, and the *ee* values increase slightly with decreasing nanopore size of the supports (Tables 3 and 7). This means that the confinement effect not only enhances the chiral recognition between chiral Mn(salen) and styrene (ee_{fac}), but also probably restricts the rotation of the intermediate (decreasing *trans* %) for the heterogeneous asymmetric epoxidation of styrene.

In fact, it has reported that the heterogeneous Mn(salen) catalysts significantly restrict the rotation of the intermediate and increase the *cis*/*trans* ratio of epoxides for the asymmetric epoxidation of *cis*-β-methylstyrene [14,26]. Hutchings et al. also reported that the Mn(salen) catalyst anchored in nanopores can increase the ratio of cis-epoxide for the heterogeneous asymmetric epoxidation of (*Z*)-stilbene [22]. The increased linkage length or decreased nanopore size reduces the reaction space in the nanopores and strengthens the confinement effect, which increases the ee_{fac} and *cis* % for the asymmetric epoxidation of styrene. In contrast, Mn(salen) catalysts anchored onto the external surface of MCM(1.6) without the confinement effect give constant *ee* values. The confinement effect originating from the nanopores not only enhances chiral recognition, but also restricts the rotation of the intermediate, which increases the enantioselectivity for asymmetric epoxidation.

5. Conclusion

Chiral Mn(salen) complexes were immobilized in the nanopores of AS(9.7), SBA(7.6), and MCM(2.7) and on the external surface of MCM(1.6) via phenyl sulfonic groups with varying linkage lengths. These heterogeneous catalysts show high activity and enantioselectivity for the asymmetric epoxidation of unfunctionalized olefins and give conversions, chemical selectivities, and enantioselectivities comparable to those of the homogeneous catalysts. The main results can be summarized as follows:

1. The Mn(salen) catalysts immobilized in the nanopores of supports have *ee* values that increase with increasing linkage lengths for the asymmetric epoxidation of unfunctionalized olefins, whereas the Mn(salen) catalysts anchored onto the external surface of support give almost constant *ee* values.
2. The Mn(salen) catalysts immobilized in the nanopores of AS(9.7), SBA(7.6), and MCM(2.7) show increasing *ee* values with decreasing nanopore size. These *ee* values are generally higher than those of the same catalysts immobilized on the external surface of MCM(1.6) under the same conditions.
3. The addition of PPNO to the heterogeneous Mn(salen) catalysts generally improves the activity, chemical selectivity, and enantioselectivity for the asymmetric epoxidation of nonfunctionalized olefins.
4. The heterogeneous Mn(salen) catalysts modified with methyl groups generally improve the conversion, chemical selectivity, and enantioselectivity for the heterogeneous asymmetric epoxidation of olefins.
5. The confinement effect originating from nanopores not only enhances the chiral recognition of chiral Mn(salen) catalyst, but also restricts the rotation of the intermediate, resulting in higher *ee* values than those obtained for the same catalysts anchored on the external surface.

Acknowledgments

Financial support was provided by the National Natural Science Foundation of China (grant 20321303). We thank Dr. Jianliang Xiao, University of Liverpool for helpful discussions.

References

[1] W. Zhang, J.L. Loebach, S.R. Wilson, E.N. Jacobsen, J. Am. Chem. Soc. 112 (1990) 2801.
[2] R. Irie, Y. Ito, T. Katsuki, Synlett (1991) 265.
[3] M. Palucki, P.J. Pospisil, W. Zhang, E.N. Jacobsen, J. Am. Chem. Soc. 116 (1994) 9333.
[4] E.N. Jacobsen, W. Zhang, A.R. Muci, J.R. Ecker, L. Deng, J. Am. Chem. Soc. 113 (1991) 7063.
[5] B.D. Brandes, E.N. Jacobsen, J. Org. Chem. 59 (1994) 4378.
[6] B.D. Brandes, E.N. Jacobsen, Tetrohydron Lett. 36 (1995) 5123.
[7] C.E. Song, S.G. Lee, Chem. Rev. 102 (2002) 3495.
[8] P. Mcmorn, G.J. Hutchings, Chem. Soc. Rev. 33 (2004) 108.
[9] C. Li, Catal. Rev.-Sci. Eng. 46 (2004) 419.
[10] X.G. Zhou, X.Q. Yu, J.S. Huang, S.G. Li, L.S. Li, C.M. Che, Chem. Commun. (1999) 1789.
[11] G.J. Kim, J.H. Shin, Tetrahedron Lett. 40 (1999) 6827.
[12] S. Xiang, Y.L. Zhang, Q. Xin, C. Li, Chem. Commun. (2002) 2696.
[13] V. Ayala, A. Corma, M. Iglesias, J.A. Rincón, F. Sánchez, J. Catal. 224 (2004) 170.
[14] H.D. Zhang, S. Xiang, J.L. Xiao, C. Li, J. Mol. Catal. A: Chem. 238 (2005) 175.
[15] R.I. Kureshy, I. Ahmad, N.H. Khan, S.H.R. Abdi, S. Singh, P.H. Pandia, R.V. Jasram, J. Catal. 235 (2005) 28.
[16] C. Baleizão, B. Gigante, H. Garcia, A. Corma, J. Catal. 221 (2004) 77.
[17] J.M. Fraile, J.I. García, J. Massam, J.A. Mayoral, J. Mol. Catal. A: Chem. 136 (1998) 47.
[18] R.I. Kureshy, N.H. Khan, S.H.R. Abdi, I. Ahmael, S. Singh, R.V. Jasra, J. Catal. 221 (2004) 234.
[19] S. Bhattacharjee, J.A. Anderson, Chem. Commun. (2004) 554.
[20] S. Bhattacharjee, T.J. Dines, J.A. Anderson, J. Catal. 225 (2004) 398.
[21] P. Piaggio, C. Langham, P. McMorn, D. Bathell, P.C.B. Page, F.E. Hancock, C. Sly, G.J. Hutchings, J. Chem. Soc., Perkin Trans. 2 (2000) 143.
[22] P. Piaggio, P. McMorn, D. Murphy, D. Bathell, P.C.B. Page, F.E. Hancock, C. Sly, O.J. Kerton, G.J. Hutchings, J. Chem. Soc., Perkin Trans. 2 (2000) 2008.
[23] C. Schuster, E. Möllmann, A. Tompos, W.F. Hölderich, Catal. Lett. 74 (2001) 69.

[24] C. Baleizão, B. Gigante, D. Das, M. Alvaro, H. Garcia, A. Corma, Chem. Commun. (2003) 1860.
[25] C. Baleizão, B. Gigante, D. Das, M. Alvaro, H. Garcia, A. Corma, J. Catal. 223 (2004) 106.
[26] H.D. Zhang, S. Xiang, C. Li, Chem. Commun. (2005) 1209.
[27] W. Zhang, E.N. Jacobsen, J. Org. Chem. 56 (1991) 2296.
[28] J.F. Larrow, E.N. Jacobsen, J. Org. Chem. 59 (1994) 1939.
[29] A. Hecked, D. Seebach, Helv. Chim. Acta. 85 (2002) 913.
[30] C.W. Jones, K. Tsuji, M.E. Davis, Nature 393 (1998) 52.
[31] S.H. Zhao, P.R. Ortiz, B.A. Keys, K.G. Davenport, Tetrahedron Lett. 37 (1996) 2725.
[32] B.B. De, B.B. Lohray, S. Sivaram, P.K. Tetrahedron: Asymmetry 6 (1995) 2105.
[33] S. Chang, J.M. Galvin, E.N. Jacobsen, J. Am. Chem. Soc. 116 (1994) 6937.
[34] J.F. Lorrow, E.N. Jacobsen, Top. Organomet. Chem. 6 (2004) 123.
[35] H.D. Zhang, Y.M. Zhang, C. Li, Tetrahedron: Asymmetry 16 (2005) 2417.
[36] J.M. Thomas, T. Maschmeyer, B.F.G. Johnson, D.S. Shephard, J. Mol. Catal. A 141 (1999) 139.
[37] M.D. Jones, R. Raja, J.M. Thomas, B.F.G. Johnson, Top. Catal. 25 (2003) 71.
[38] S. Taylor, J. Gullick, P. McMorn, D. Bethell, P.C.B. Page, F.E. Hancock, F. King, G.J. Hutchings, J. Chem. Soc., Perkin Trans. 2 (2001) 1714.
[39] N.A. Caplan, F.E. Hancock, P.C.B. Page, G.J. Hutchings, Angew. Chem. Int. Ed. 43 (2004) 1685.